

Das Wiedererwachen des Zweitakt Gegenkolben Dieselmotors für Nutzfahrzeuge

The Renaissance of the Opposed-Piston Two-Stroke Diesel Engine for Commercial Applications

Gerhard Regner, Randy Herold, Michael Wahl,
James Lemke, Fabien Redon, Eric Dion

Achates Power, Inc.
4060 Sorrento Valley Boulevard
San Diego, CA 92121, USA



Abstract

Historically, the opposed-piston two-stroke diesel engine set combined records for fuel efficiency and power density that have yet to be met by any other engine type. In the latter half of the twentieth century, the advent of modern emissions regulations stopped the wide-spread development of two-stroke engines for on-highway use. At Achates Power, modern analytical tools, materials, and engineering methods have been applied to the development process of an opposed-piston two-stroke engine, resulting in an engine design that has demonstrated a more than 18% fuel consumption improvement compared to a state-of-the-art medium-duty diesel engine at US EPA 2010 tail-pipe emissions levels. In addition, a development roadmap is presented that corroborates the upside potential of this engine architecture to reach 49.5% brake thermal efficiency in future applications.

Kurzfassung

Hinsichtlich des Kraftstoffverbrauchs und der Leistungsdichte hat der Zweitakt Gegenkolben Dieselmotor schon in der Vergangenheit Rekorde aufgestellt, die bis heute noch von keiner anderen Motorenkonfiguration erreicht wurden. Die Evolution der modernen Emissionsgesetzgebung hat in der zweiten Hälfte des zwanzigsten Jahrhunderts die Weiterentwicklung des Zweitakt Motors für Strassenanwendungen weitgehend gestoppt. Jedoch mit dem Einsatz moderner Materialien, Berechnungs- und Konstruktionsmethoden im Entwicklungsprozess hat das Achates Power Motorenkonzept eine mehr als 18 %ige Verbesserung des Kraftstoffverbrauchs verglichen zu einem hochmodernen Medium-Duty Dieselmotor für US EPA 2010 Abgasemissionsgesetzgebung demonstriert. Zusätzlich wird ein Weiterentwicklungsplan vorgestellt, der das Potenzial dieser Motorenbauart aufzeigt und einen thermischen Wirkungsgrad von 49.5 % für zukünftige Anwendungen erwarten lässt.

1. INTRODUCTION

Opposed-piston two-stroke engines were conceived in the late 1800s in Europe and subsequently developed in multiple countries for a wide variety of applications [1-3]. An excellent summary of the history of opposed-piston engines can be found in [1]. Produced initially for their manufacturability, high power density, and competitive fuel efficiency, opposed-piston two-stroke engines demonstrated their versatility in a variety of applications including aircraft, ships, tanks, trucks, power generation and locomotives and maintained their presence throughout most of the twentieth century. Historically, all types of engines have faced a number of technical challenges related to emissions, fuel efficiency, cost and durability – to name a few – and these challenges have been more easily met by four-stroke engines, as demonstrated by their widespread use today. However, the limited availability of fossil fuels and the corresponding rise in fuel cost has led to a re-examination of the fundamental limits of fuel efficiency in internal combustion (IC) engines, and opposed-piston engines, with their inherent thermodynamic advantage, have emerged as a promising alternative. This paper discusses the potential of opposed-piston two-stroke engines in light of today's market and regulatory requirements, the performance and emissions results obtained at operating conditions consistent with a medium-duty application, and the upside potential of this engine architecture by means of a brake thermal efficiency roadmap.

A number of fundamental advantages of opposed-piston two-stroke engines make them attractive alternatives to common four-stroke engines. The opposed-piston (OP) arrangement, characterized by two pistons reciprocating opposite to each other in a common cylinder, has inherent heat transfer benefits compared to a standard crank-slider arrangement with a single piston and a cylinder head, and these benefits can be realized without sacrifices to engine friction or mechanical durability. First, the OP architecture creates a larger cylinder displacement for a given cylinder bore diameter, leading to a reduction in the number of cylinders compared to an engine with a standard crank-slider/cylinder head arrangement. A reduced number of cylinders decreases the surface area available for in-cylinder heat transfer. Second, an effective stroke-to-bore ratio in the range of 2:1 to 2.5:1 can be realized without increasing the piston speed, leading to more favorable surface-area-to-volume ratios and a further reduction of in-cylinder heat transfer. Third, the OP arrangement eliminates the cylinder head and replaces it with a second piston that can be maintained at a higher metal temperature, reducing the thermal losses to that surface of the combustion chamber. A quantitative assessment of how all these effects contribute to a fundamental thermodynamic advantage can be found in [4].

The two-stroke cycle and its double firing frequency gives engine designers the choice of decreasing brake mean effective pressure (BMEP) levels and increasing power density compared to four-stroke engines of equivalent power output. The lower BMEP levels can be accomplished with lower peak cylinder pressures and therefore lower peak cylinder temperatures, both of which lead to design advantages. The lower cylinder pressures result in lower mechanical stress on engine components and therefore can be designed to be of lighter weight. The lower cylinder temperatures result in decreased NO_x formation during combustion, lowering the requirements for exhaust gas recirculation (EGR) and/or NO_x aftertreatment devices. The increased power density leads directly to smaller engine package size and weight, both of which are beneficial to increasing overall vehicle fuel economy and to decreasing manufacturing costs.

1.1. MODERN SOLUTIONS TO OPPOSED-PISTON TWO-STROKE ENGINE CHALLENGES

Thanks to modern development tools and advanced fuel systems, the OP architecture with a liner-mounted injector has turned from a technical challenge into a unique opportunity. The availability of fuel systems with high injection pressures and the greater ease of manufacturing asymmetric injector nozzle hole directions have enabled the fuel spray of liner-mounted injectors to better utilize the air within the combustion chamber with little-to-no wall impingement. Additionally, the ability to quickly and accurately model the fuel spray, in-cylinder gas motion, and combustion using computational fluid dynamic (CFD) software packages (e.g. [5], [6]) has allowed the engineering of the combustion chamber geometry and nozzle configuration to achieve clean and efficient combustion, as demonstrated by the results reported in this paper. The ability to shape two combustion chamber surfaces (the two pistons crowns) and incorporate multiple fuel injection locations on the liner has provided a larger design space than is available in common four-stroke engines.

With regards to emissions, one of the opportunities afforded by the two-stroke scavenging process is the ability to retain some portion of the burnt charge in the cylinder after combustion (“internal” EGR) as a means to control NO_x by simply reducing the pumping work applied by the aircharge system. For high rates of EGR, the use of cooled external EGR is still required, but the engine’s supercharger provides an efficient method to pump the EGR from the exhaust to the intake [4].

1.2. THE RENAISSANCE OF THE OPPOSED-PISTON TWO-STROKE ENGINE

The renaissance of the opposed-piston two-stroke engine has been aided by three circumstances: the increasing demand and regulatory requirements for highly fuel-efficient and clean internal combustion engines, the thermal efficiency benefit of OP engines that is not found with other engine architectures, and the development of designs that have overcome the challenges and limitations of previous implementations. The fundamental thermal efficiency benefits of this engine along with its low emissions, small package size and weight, and low cost relative to current four-stroke engines make it an attractive alternative for future commercial and passenger vehicles. The following sections summarize the performance and emissions results of an Achates Power opposed-piston two-stroke engine that meets low engine-out emissions levels with acceptable oil consumption while achieving fuel consumption levels that exceed those of the current state-of-the-art four-stroke engine.

2. DATA ACQUISITION AND CORRELATION

2.1. SINGLE CYLINDER RESEARCH ENGINE

The custom single-cylinder research engine, shown in Figure 1, has been manufactured in-house and is tested on a 300 hp AC dynamometer. The engine has a trapped nominal compression ratio of 16.7, a bore of 80 mm, and a stroke of 212.8 mm, resulting in a displaced volume of 1.06 L. The liner geometry creates a fixed port timing, and the piston geometry and injection spray pattern have been specified based on analytical combustion simulation results. A variable swirl device is installed on the intake end of the cylinder to have continuous control over the in-cylinder swirl ratio. The used common-rail fuel injection system is capable of injection pressures up to 2000 bar

and can produce multiple injection events per engine cycle. In the current design, the single-cylinder research engine is limited to a maximum cylinder pressure of 160 bar and a maximum liner temperature of 200 °C.

The conditioned combustion air and EGR are delivered to the intake manifold of the single-cylinder engine via the system shown in Figure 2. An external air compressor feeds compressed air to the conditioning unit where it is mixed with exhaust gas taken from the exhaust side of the engine. An EGR pump, necessary because of the required pressure difference across the cylinder, pulls the exhaust through a gas-to-water heat exchanger before delivering exhaust gas to the intake stream. The EGR rate delivered to the engine is controlled by the EGR pump speed and a ball valve located downstream of the pump. After the air and exhaust gas are mixed, the intake gas flows through a second heat exchanger followed by a heater to precisely control the intake manifold temperature. The exhaust manifold pressure is set with a back pressure valve in the exhaust system.

In-cylinder pressure was measured at 0.5° crank-angle resolution with a Kistler 6052C piezoelectric pressure transducer coupled to a Kistler 5064 charge amplifier. The cylinder pressure signal is pegged to an average of the intake and exhaust manifold pressures, measured with Kistler 4005B and 4049A high-speed pressure transducers, respectively. Custom in-house software is used to acquire and process the data. A California Analytical Instruments (CAI) emissions analyzer is used to measure the steady-state concentration of five exhaust species (CO₂, CO, O₂, HC, NO_x) and intake CO₂. A Dekati DMM-230A Mass Monitor provided real-time particulate matter values, and an AVL 415s Smoke Meter provides a measure of exhaust soot content. A measurement of the combustion noise is provided by an AVL FlexIFEM Advanced Noise Meter.

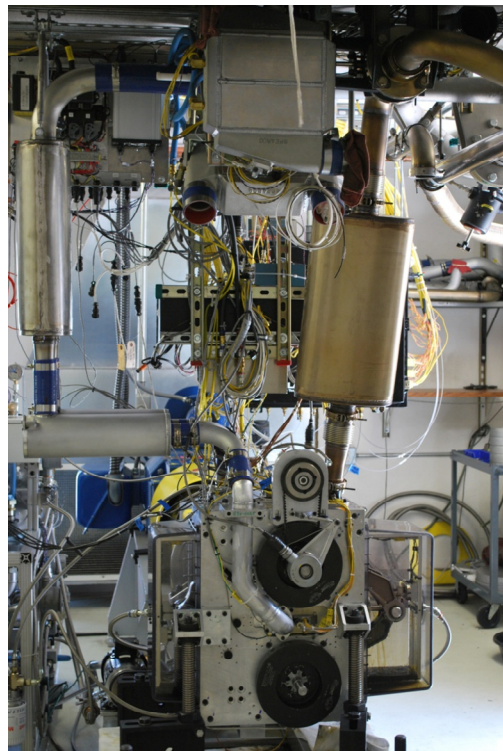


Figure 1: Single cylinder research engine installed in test cell

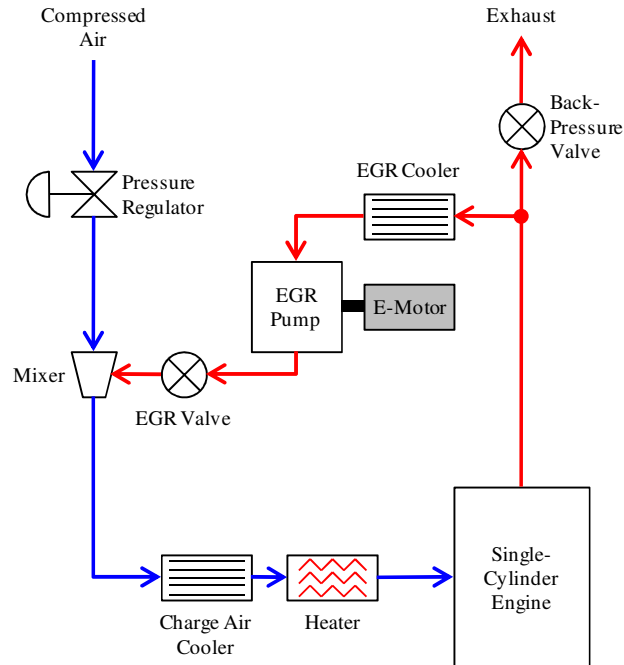


Figure 2: Schematic of the air and EGR conditioning system

2.2. INTERFACE MODEL

Friction and pumping energy losses, which represent the difference between indicated work and brake work, are specific for each engine configuration and do not translate from a single-cylinder to a multi-cylinder engine by simple multiplication. In order to predict the brake-specific performance of a multi-cylinder engine based on single-cylinder combustion results, an “interface model” has been created in 1D engine system simulation software. This model is correlated to the in-cylinder pressure trace so as to provide multi-cylinder-based predictions of the friction and pumping work required at the operating point measured on the dynamometer. The results from the interface model therefore provide predictions of multi-cylinder brake-specific performance and emissions parameters based on measured single-cylinder results.

Figure 3 shows the schematic of the input data and assumptions of the interface model. The combustion chamber geometry, the piston motions, and the porting profiles are identical to what exists in the single-cylinder engine, while the number of cylinders and associated manifold configurations are application specific. Engine speed, fuel flow rate, air flow rate, EGR percentage, cylinder pressures at intake port closing (IPC), and intake manifold temperatures match the measured values. The rate of heat release is derived from the measured cylinder pressure and is input directly into the combustion sub-model. Assumptions for the air-handling equipment, charge cooling components, and aftertreatment system are used in the pumping loss prediction. The Chen-Flynn mechanical friction model is based on the mechanism design and analysis and is correlated to experimental friction results. The work needed to drive all accessories, including the supercharger, is also taken into account.

The interface model air-handling system (Figure 4) consists of a supercharger, a turbocharger, and a charge air cooler after each compression stage. The size and characteristics of the air-handling

system components are application specific. The compressor and turbine are modeled as ‘mapless’ components with user-specified efficiencies that are consistent with the operating point and available turbocharger supplier data, and the supercharger model uses a full map obtained from a supplier. A dual-drive-ratio mechanism is assumed for the engine-supercharger connection. The two drive ratios for the supercharger are useful for maintaining high thermal efficiency over the entire engine map, for increasing low speed torque, and for enhancing the cold start capability of the engine. A supercharger recirculation loop and valve are included to control the inlet manifold pressure, and a turbine waste-gate valve is modeled for over-boost and over-speed protection, although at the conditions provided here the waste-gate valve is not needed.

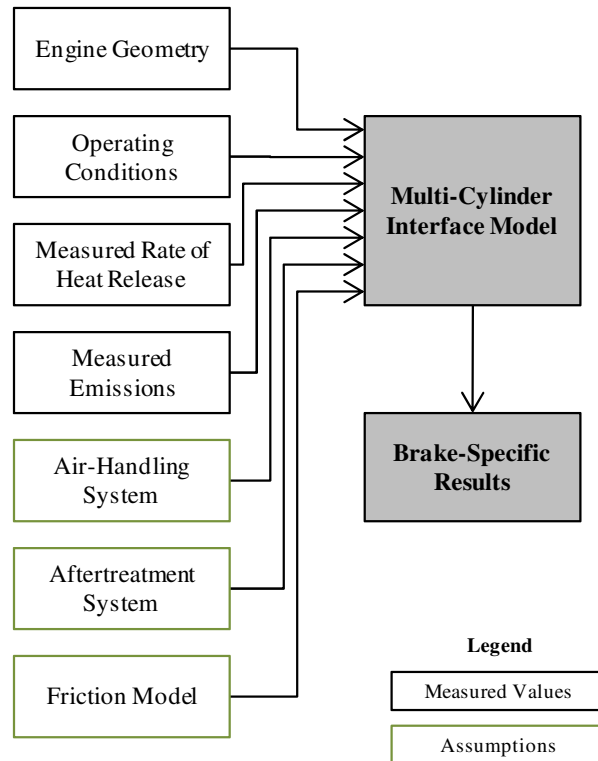


Figure 3: Multi-cylinder interface model input data flow

EGR is introduced into the intake system after the compressor and before the first charge air cooler. It is assumed that both charge air coolers are of the air-to-water type and are located on a secondary low temperature coolant circuit. The charge air coolers' effectiveness values are set to 90%, which is a valid assumption even with a certain degree of cooler fouling. Charge air cooler fouling with this arrangement is expected to be less pronounced than in four-stroke engines. The hot EGR mixes with cooler compressor outlet air prior to entering the charge air cooler, which significantly reduces the inlet charge temperature and the soot concentration thereby decreasing the likelihood of fouling [7]. The second charge air cooler is assumed to be mounted close to the intake manifold in a high position to avoid condensate build-up in the cooler and the associated corrosion. Concerns about hydrolock associated with condensate build-up are decreased with an opposed-piston two-stroke engine because, in configurations of three cylinders or more, at least one of the cylinders will always be open to both manifolds, allowing the condensate to flow through the engine.

The interface model requires a detailed characterization of the scavenging process because it is important to arrive at the correct concentrations of fresh air and residual gas in the cylinder prior to the start of the closed-cycle portion of the simulation. For this reason, the scavenging efficiency was measured in the engine using an in-cylinder CO₂ sampling method [8], and the scavenging efficiency versus delivery ratio relationship was used in the interface model correlation process.

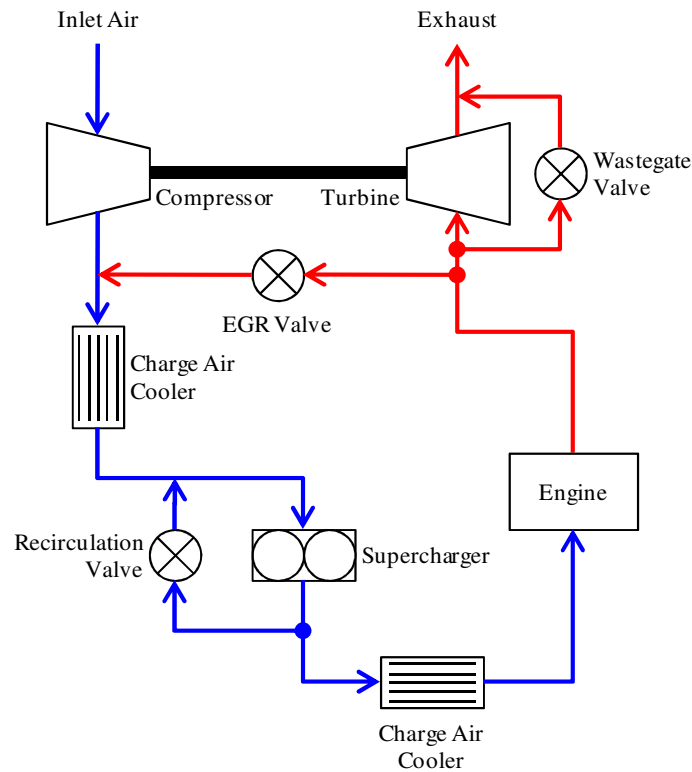


Figure 4: Air handling system configuration

The interface model was exercised by first setting a turbine effective diameter and the supercharger mechanical drive ratios. Then for each operating condition, the compressor and turbine efficiencies were specified based on supplier data, and the two-stroke scavenging schedule was set to match measured results at the given speed and delivery ratio. Finally, the cylinder pressure trace, intake air flow per cylinder, and EGR percentage were matched to experimental results when using the measured rate of heat release by adjusting the following parameters: supercharger drive ratio (to one of the two possible values), supercharger recirculation valve, and EGR valve position. If a sufficient match to the experimental results could not be achieved, a new set of boundary conditions was provided to the single cylinder engine, the experiment was re-run with the new operating condition, and the interface model was re-matched to the updated experimental results. This iterative process typically succeeded within two to three iterations. The results of this correlation exercise provided a prediction of the brake specific parameters assuming a fixed turbine size and a dual-drive-ratio supercharger.

3. RESULTS

3.1. MEDIUM-DUTY ENGINE PERFORMANCE

The process of measuring single-cylinder combustion results and then using the interface model to predict multi-cylinder engine performance has been exercised for an operating range typical of an engine in a medium-duty commercial vehicle. The specifications of this medium-duty engine are provided in Table 1. It should be noted that although the total engine power output for a three-cylinder, 1.06 L per cylinder engine would be slightly underpowered for a typical medium-duty application, the three-cylinder engine is the preferred configuration for thermal efficiency considerations and therefore was used in this study. Scaling this engine to a larger displacement per cylinder would not only increase the power but further improve the thermal efficiency, as will be discussed later. The engine operating conditions, designated as A25, A75, B50, B75, C25, and C75 are derived from the steady-state supplemental certification cycle adopted by the US and Europe [9]. Only 6 of the 13 engine modes are considered as a representative subset for measuring fuel consumption and emissions in order to reduce total testing time. The same weighting factors as specified by the legislation are used to calculate the cycle-average fuel consumption and emissions values.

Table 1: Medium-Duty Engine Specifications

Maximum Power	47 kW/cylinder @ 2400 rpm
Maximum Torque	240 Nm/cylinder @ 1600 rpm
Number of Cylinders	3
Displaced Volume	1.06 L/cylinder
Stroke	212.8 mm
Bore	80 mm
Maximum BMEP	13.6 bar
Trapped Compression Ratio	16.7:1

Table 2 provides performance and emissions results for the Achates Power opposed-piston two-stroke medium-duty engine, where the indicated results were measured directly in the single-cylinder research engine, and the brake-specific performance values were based on the multi-cylinder interface-model predictions for friction and pumping losses. The operating conditions were selected based on the assumption that a Vanadium SCR catalyst, which typically has a NO_x conversion efficiency of over 90 % in a temperature range between 300 and 400 °C, was used as the NO_x aftertreatment device.

The peak brake thermal efficiency of 44.5 %_{fuel} occurs at the B75 operating condition and is equivalent to achieving a brake-specific fuel consumption of 188.2 g/kWh. The A75, B50, and C75 operating conditions are also highly efficient, with brake thermal efficiencies in excess of 40 %_{fuel}. The low-load A25 and C25 conditions are less efficient because of higher relative frictional losses. The engine out brake-specific NO_x emissions at B75 is 2.1 g/kWh with a turbine outlet temperature predicted to be 365 °C, and the brake specific soot emission at B75 is 0.039 g/kWh.

Table 2: Achates Power opposed-piston two-stroke engine performance and emissions results

Engine Condition		A25	A75	B50	B75	C25	C75
Engine Speed	rpm	1600	1600	2000	2000	2400	2400
IMEP	bar	3.6	10.8	7.1	10.3	4.1	9.9
BMEP	bar	2.9	9.1	6.0	9.1	2.9	8.2
Indicated Power	kW	31.3	93.1	76.6	109.8	53.1	126.7
Brake Power	kW	24.7	78.5	64.8	96.9	37.6	104.8
Ind. Thermal Efficiency	% _{fuel}	50.6	49.8	51.9	50.5	52.6	51.4
Brake Thermal Efficiency	% _{fuel}	40.1	41.9	43.9	44.5	37.2	42.5
Friction Losses	% _{fuel}	8.9	3.6	6.3	4.6	12.2	5.8
Pumping Losses	% _{fuel}	1.7	4.3	1.6	1.4	3.2	3.1
Exhaust + Heat Losses	% _{fuel}	49.4	50.2	48.1	49.5	47.4	48.6
Turbine Outlet Temperature	°C	287	312	325	364	303	345
ISFC	g/kWh	165.6	168.3	161.5	166.0	159.2	163.1
BSFC	g/kWh	209.1	199.9	190.7	188.2	225.0	197.1
BSNO _x	g/kWh	1.85	2.59	2.29	2.10	2.24	2.33
BSSoot	g/kWh	0.008	0.008	0.016	0.039	0.026	0.026
BSCO	g/kWh	0.40	0.20	0.30	0.56	0.96	0.96
BSHC	g/kWh	0.61	0.26	0.40	0.41	0.35	0.35

The cycle-averaged brake-specific fuel consumption (BSFC) and emissions values are provided in Table 3. The cycle-averaged BSFC of 195.3 g/kWh is achieved with BSNO_x emissions equal to 2.25 g/kWh and BSSoot emissions equal to 0.03 g/kWh. The engine-out emissions are in a range that allows 2010 US tailpipe emission requirements [10] to be met with typical aftertreatment (DOC, DPF, SCR) performance.

Table 3: Cycle-averaged brake-specific fuel consumption and emissions values for the Achates Power engine and a state-of-the-art medium-duty four-stroke engine [11]. Note that only NO_x emission were provided for the reference engine.

Engine Condition		Achates Power	Ref. [11]
BSFC	g/kWh	195.3	239.9
BSNO _x	g/kWh	2.25	1.30
BSSoot	g/kWh	0.03	---
BSCO	g/kWh	0.60	---
BSHC	g/kWh	0.40	---

Also included in Table 3 are cycle-averaged BSFC and NO_x emission values from a state-of-the-art, medium-duty four-stroke engine [11]. The cycle-averaged values from the four-stroke engine were averaged over the same six operating conditions as the Achates Power engine. The Achates Power engine has 18.6% lower BSFC than the reference four-stroke engine, albeit at a higher engine-out NO_x emission level. Because the reference four-stroke engine did not provide soot

emission numbers, it is impossible to determine how much of the fuel consumption advantage would be sacrificed to achieve the same NOx emissions.

Oil consumption in a two-stroke engine is a critical aspect for achieving emissions compliance and historically difficult to achieve. In this case, the fuel specific oil consumption was measured to be less than 0.1% for a majority of the engine speed/load map, as detailed in reference [12].

4. BRAKE THERMAL EFFICIENCY ROADMAP FOR THE FUTURE

The Achates Power opposed-piston two-stroke engine has demonstrated brake thermal efficiency (BTE) of 44.5 % (see Table 2) with engine hardware and calibration that are still in an early stage of development. Higher engine thermal efficiencies will be achieved through hardware and calibration improvements, some of which are unique to the Achates Power engine architecture and some of which are industry-wide advancements. To quantify the effect of these possible improvements, a BTE roadmap has been developed. The potential efficiency improvements are estimated based on internal analysis as well as findings from a recent report on fuel economy technologies to the United States National Academy of Sciences [14]. Figure 9 shows the energy balance and efficiency improvements using the B50 results from Table 2 as a baseline. The B50 operating condition was selected for the baseline because it more closely represents a standard road-load operating condition for heavy-duty truck engines.

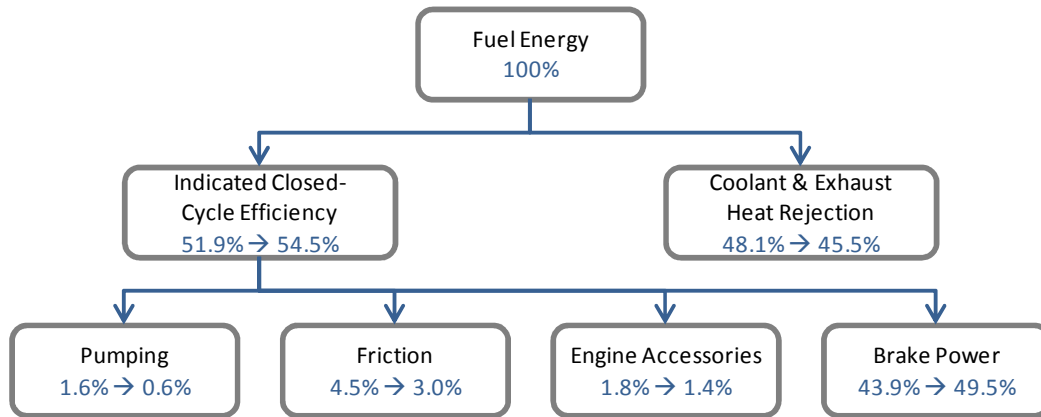


Figure 9: Energy balance and efficiency improvements at B50 load point

In order to achieve a brake thermal efficiency of 49.5%, the indicated closed-cycle efficiency, the pumping work, the mechanical friction, and the power consumption of the engine accessories all require further improvements. A detailed discussion of each improvement opportunity can be found in the following sections to support the quantitative estimates put forth in Figure 9.

4.1. Indicated Closed Cycle Efficiency

The ability to convert fuel energy to mechanical energy efficiently and cleanly while still meeting external mechanical and emission constraints is paramount to a successful internal combustion engine. For the current B50 status, a gross indicated thermal efficiency of 51.9% is achieved using a calibration with a maximum of 5 bar/deg maximum pressure rise rate, and a greater than 90%

efficient SCR device that allows US 2010 emissions requirements to be met with 2 g/hp-hr engine-out NOx.

Increasing the indicated thermal efficiency is a primary step toward increasing the brake thermal efficiency. In the present analysis, the effects of changes to the assumed engine hardware and calibration on indicated thermal efficiency were evaluated using a custom 0D closed-cycle analysis tool, described in detail in reference [4]. As a starting point, the engine displacement was increased from the current engine hardware to the 4.9L, three-cylinder engine configuration. By doing so, not only was the engine power output increased to be compatible with a medium-duty engine, but the larger cylinder displacement also resulted in an increase of $0.6\%_{\text{fuel}}$ in indicated thermal efficiency without any other hardware or calibration changes. The increased cylinder size results in a more favorable area-to-volume ratio that reduces the in-cylinder heat transfer and allowed more of the fuel energy to be converted to work.

To further increase the indicated thermal efficiency, some of the external engine constraints were relaxed: the assumed maximum cylinder pressure was increased and the NOx conversion efficiency of the SCR aftertreatment device was assumed to increase through continued innovation and development. By relaxing these two constraints, the engine compression ratio could be increased because the higher cylinder pressures and temperatures that result from an increased compression ratio could be withstood. By increasing the trapped compression ratio by 4.5 compression ratio units, an increase in indicated thermal efficiency of $1.5\%_{\text{fuel}}$ was realized.

In order to maintain the pressure rise rate within the 5 bar/deg limits when the compression ratio was increased, changes to the combustion shape became necessary. By assuming a combination of higher quality fuel injection equipment, better combustion control that allows for more sophisticated combustion regimes, and improved in-cylinder mixing during combustion, the combustion duration was reduced by approximately 2.8 degrees and the premixed-burn spike was decreased. This optimized combustion resulted in an indicated thermal efficiency increase of $0.5\%_{\text{fuel}}$.

The combination of increased displacement, increased compression ratio, and optimized combustion improved the indicated thermal efficiency by $2.6\%_{\text{fuel}}$, as detailed in Figure 10.

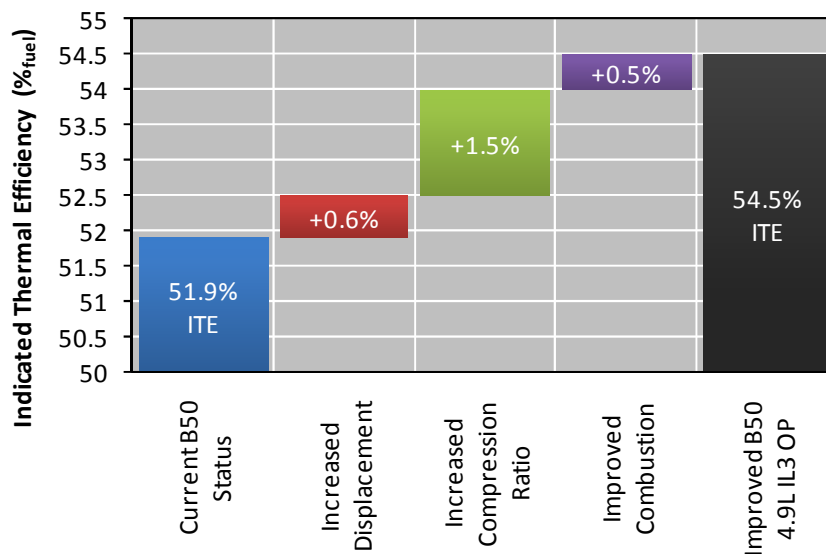


Figure 10: Future indicated closed cycle efficiency improvements for the B50 load point

4.2. Gas Exchange

Gas exchange losses for a two-stroke engine are represented by the pumping work provided by the crankshaft driven supercharger. The mechanical losses to drive the supercharger are included in the accessory power consumption and will be discussed in the next section. In general, the supercharger power requirements depend on the pressure losses of the entire air system, the additional pumping to compensate for short-circuiting of air during scavenging, the EGR rate, and the efficiencies of super- and turbocharger. All these effects were quantified by a 1D engine performance simulation tool with results shown in Figure 11. The leftmost bar represents the baseline B50 condition with pumping losses equivalent to $1.63\%_{\text{fuel}}$ as shown in Table 3.

Several measures were applied in succession to reduce the pumping work. First, the porting arrangement was optimized for the B50 load point leading to a 4% improvement in the scavenging efficiency. An increase in scavenging efficiency reduces the need for additional pumping to achieve the same delivery ratio and trapped air mass, thereby reducing the pumping work by $0.4\%_{\text{fuel}}$. The improved scavenging also implies less short-circuiting of cold air through the exhaust ports which increases the average exhaust temperature by $16\text{ }^{\circ}\text{C}$, a change that is helpful in maintaining high aftertreatment conversion efficiencies.

Second, it was assumed that the improved NOx conversion efficiency in the aftertreatment system, as discussed previously, allows for an additional reduction of the external EGR rate by 5% for the same tail pipe NOx emissions. As a result, the pumping losses reduce by another $0.18\%_{\text{fuel}}$ while increasing the exhaust temperature an additional $13\text{ }^{\circ}\text{C}$. The combination of more efficient scavenging and reduced external EGR increased the exhaust temperatures nearly $30\text{ }^{\circ}\text{C}$ while reducing pumping work $0.57\%_{\text{fuel}}$.

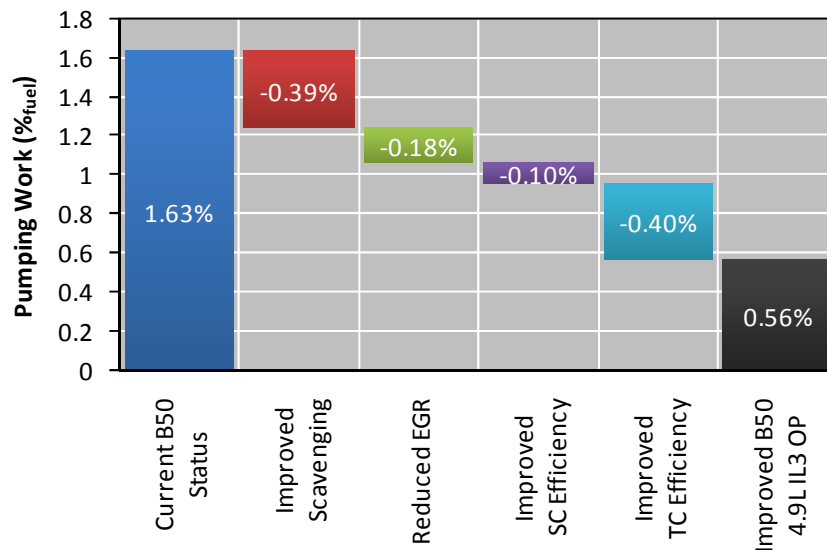


Figure 11: Future pumping work reductions for the B50 load point

As previously mentioned, this roadmap assumes a migration from the current 3.2 liter to a 4.9 liter displacement to meet the power and torque requirements of a specific medium-duty application. The larger displacement with increased mass flow rate naturally leads to larger super- and turbochargers with better efficiencies. For a 3% isentropic efficiency improvement for both super-

and turbocharger, the pumping losses reduce by a combined 0.50% of fuel, with a larger contribution coming from the turbocharger since the turbocharger compressor provides a majority of the pumping work required at the B50 operating condition.

4.3. Friction and Engine Accessories

Engine friction and accessory power consumption play a pivotal role with regards to the maximum achievable BTE and need to be carefully managed to ensure a competitive engine performance. Since engine friction is architecture specific, an engine with a dual crank slider mechanism (similar to a Jumo 205/207 [1]) was subjected to a friction strip down test and correlated to a friction model. The power consumption of the fuel and oil pumps was also measured whereas the alternator, water pump and supercharger friction was derived from vendor information and literature. The resulting friction breakdown at the B50 load condition for a 4.9L IL3 OP engine is shown in Figure 12. The friction breakdown of an OP engine is similar to that of a conventional 4-stroke engine with the exception of the missing valvetrain in the case of an OP engine [13].

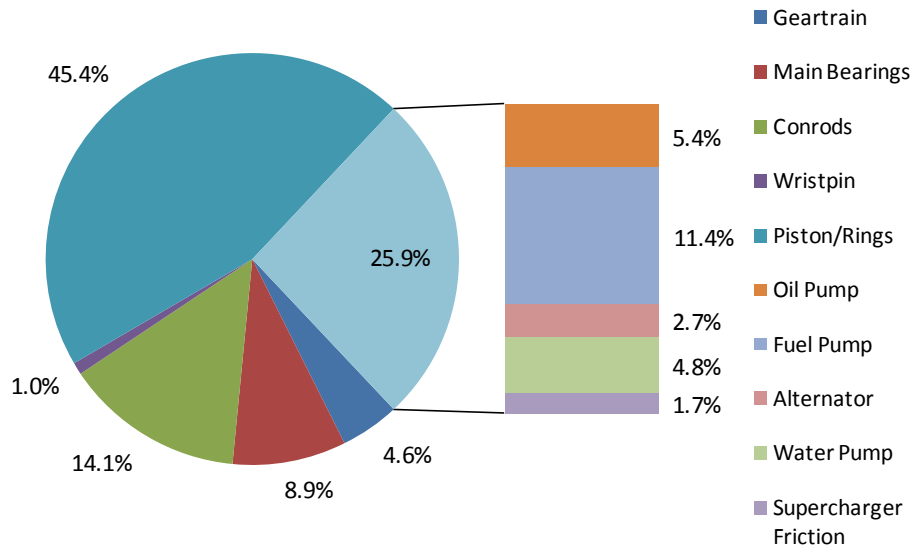


Figure 12: Friction breakdown of a 4.9L IL3 OP engine for the B50 load point

As can be seen from Figure 12, the power cylinder friction (ring/liner and piston/liner friction) is the largest contributor to overall friction which, not surprisingly, closely matches the situation in a 4-stroke diesel engine since both engine types employ a slider-crank mechanism. It is therefore a reasonable strategy to leverage the same industry-wide advancements in the area of tribology and advanced lubricants to lower the friction losses of the power cylinder in an OP engine. Specific guidance on the effectiveness of various friction reduction measures can be found on pages 4-15 ff. in reference [14] suggesting efficiency gains of at least $1\%_{\text{fuel}}$ and potentially up to $2\%_{\text{fuel}}$. For this roadmap, the friction reduction for power cylinder, bearings and geartrain are projected to divide up as follows (see Figure 13): $0.9\%_{\text{fuel}}$ are gained from the power cylinder based on further optimization of the ring and piston skirt contours combined with advanced surface textures and/or

coatings; $0.5\%_{\text{fuel}}$ from the bearings based on size optimization and oil temperature management; and $0.1\%_{\text{fuel}}$ from the geartrain based on optimized gear tooth profiles. Combined, the projected improvements total $1.5\%_{\text{fuel}}$ and are well within the quoted range of 1 to $2\%_{\text{fuel}}$ from reference [14]. Furthermore, the indicated thermal efficiency improvements discussed previously result in reduced heat rejection to the coolant allowing for a reduction in coolant flow rates. Variable displacement pumps provide further benefits by tailoring the pump performance to better match the flow rate requirements at every load point. The resulting reduction in pumping losses for oil and water are estimated to be $0.2\%_{\text{fuel}}$ (compare with Table 3-3 in [14]).

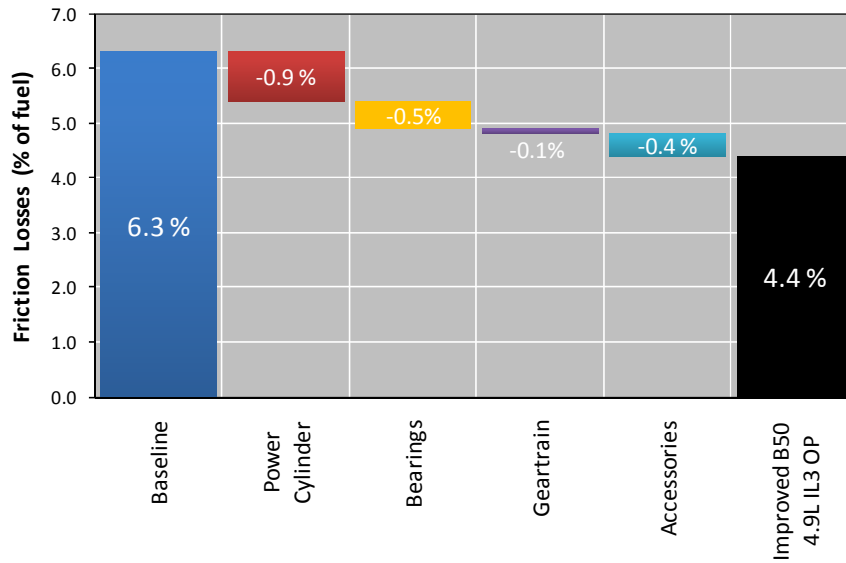


Figure 13: Future friction reductions at B50 load point

Lastly, the recent trend of electrifying accessories in conventional 4-stroke engines applies equally to OP engines. The expected benefit is estimated to be $0.2\%_{\text{fuel}}$ (compare with Table 3-3 in [14]).

By incorporating all friction reduction measures the friction losses reduce to $3.0\%_{\text{fuel}}$ and the power losses of the accessories reduce to $1.4\%_{\text{fuel}}$ of fuel energy.

5. CONCLUSIONS

The results reported in this work have shown that the opposed-piston two-stroke engine architecture is a suitable platform for a highly efficient and clean internal combustion engine featuring low oil consumption. A cycle-averaged brake-specific fuel consumption (BSFC) value of 195.3 g/kWh is achieved (188.2 g/kWh at best point) with engine-out emission levels that, when paired with existing aftertreatment technology, are expected to achieve the stringent 2010 US heavy-duty emission standards. This BSFC value is 18.6% lower than a state-of-the-art four-stroke engine designed for the same medium-duty application.

A brake thermal efficiency roadmap has been presented to illustrate the potential for further efficiency gains. The roadmap suggests that the Achates Power opposed-piston engine in a 4.9 liter 3-cylinder configuration is fundamentally capable of reaching 49.5% brake thermal efficiency.

7. REFERENCES

- [1] Pirault, J.-P. and Flint, M., Opposed Piston Engines: Evolution, Use, and Future Applications, SAE International, Warrendale, PA, 2009.
- [2] Junkers, H., “Cylinder of Internal-Combustion Engines and Other Similar Machines”, U.S. Patent 1 231 903, Jul. 3, 1917.
- [3] Junkers, H., “Engine”, U.S. Patent 2 031 318, Feb. 18, 1936.
- [4] Herold, R.E., Wahl, M.H., Regner, G., Lemke, J.U., and Foster, D.E., “Thermodynamic Benefits of Opposed-Piston Two-Stroke Engines”, SAE Technical Paper 2011-01-2216, 2011.
- [5] Amsden, A.A., “KIVA-3V: A Block-Structured KIVA Program for Engines with Vertical or Canted Valves”, Los Alamos National Laboratory report LA-13313-MS, July 1997.
- [6] Richards, K. J., Senecal, P. K., and Pomraning, E., CONVERGE™ (Version 1.3), Convergent Science, Inc., Middleton, WI, 2008.
- [7] Teng, H. and Regner, G., “Characteristics of Soot Deposits in EGR Coolers”, SAE International Journal of Fuels and Lubricants, Vol. 2, No. 2, pp. 81-90, 2010. Also published as SAE Technical Paper 2009-01-2671, 2009.
- [8] Foudray, H.Z. and Ghandhi, J.B., “Scavenging Measurements in a Direct-Injection Two-Stroke Engine”, SAE Technical Paper 2003-32-0081, 2001.
- [9] Heavy-Duty Supplemental Emissions Test (SET), Retrieved from <http://www.dieselnet.com/standards/cycles/set.php>, 2010.
- [10] Heavy-Duty Truck and Bus Engines, Retrieved from <http://www.dieselnet.com/standards/us/hd.php>, 2010.
- [11] DeRaad, S., Fulton, B., Gryglak, A., Hallgren, B., Hudson, A., Ives, D., Morgan, P., Styron, J., and Waszczenko, E., “The New Ford 6.7L V-8 Turbocharged Diesel Engine”, SAE Technical Paper 2010-01-1101, 2010.
- [12] Callahan, B.J., Wahl, M.H., and Froelund, K., “Oil Consumption Measurements For A Modern Opposed-Piston Two-Stroke Diesel Engine”, ASME Technical Paper ICEF2011-60140, 2011.
- [13] Comfort, A., “An Introduction to Heavy-Duty Diesel Engine Frictional Losses And Lubricant Properties Affecting Fuel Economy – Part I”, SAE Technical Paper 2003-01-3225, 2003.
- [14] “Assessment of Fuel Economy Technologies for Medium- and Heavy-Duty Vehicles”, Report to National Academy of Sciences, Final Report, TIAX LLC, Case D0506, 2009.